

## Article

# DFT Study on the Combined Catalytic Removal of N<sub>2</sub>O, NO, and NO<sub>2</sub> over Binuclear Cu-ZSM-5

Congru Gao, Jianwei Li \*, Jie Zhang \* and Xiuliang Sun

State Key Laboratory of Chemical Resource Engineering, Beijing University of Chemical Technology, Beijing 100029, China; gaocr@mail.buct.edu.cn (C.G.); sunxl@mail.buct.edu.cn (X.S.)

\* Correspondence: lijw@mail.buct.edu.cn (J.L.); zhangjie@mail.buct.edu.cn (J.Z.); Tel.: +86-1361-105-3831 (J.L.); +86-1800-113-7991 (J.Z.)

**Abstract:** The large amount of nitrogen oxides (N<sub>2</sub>O, NO, NO<sub>2</sub>, etc.) contained in the flue gas of industrial adipic acid production will seriously damage the environment. A designed binuclear Cu-ZSM-5 catalyst can be applied to decompose N<sub>2</sub>O and reduce NO and NO<sub>2</sub>, purifying the air environment. Using the density functional theory method, the catalytic decomposition mechanisms of N<sub>2</sub>O, NO<sub>x</sub>-NH<sub>3</sub>-SCR, and NO<sub>x</sub>-assisted N<sub>2</sub>O decomposition is simulated over the Cu-ZSM-5 model. The results indicate that N<sub>2</sub>O can be catalytically decomposed over the binuclear Cu active site in the sinusoidal channel. The speed-limiting step is the second N<sub>2</sub>O molecule activation process. After the decomposition of the first N<sub>2</sub>O molecule, a stable extra-frame [Cu-O-Cu]<sup>2+</sup> structure will generate. The subsequent discussion proved that the NO<sub>x</sub>-NH<sub>3</sub>-SCR reaction can be realized over the [Cu-O-Cu]<sup>2+</sup> active site. In addition, it proved that the decomposition reaction of NO and NO<sub>2</sub> can be carried out over the [Cu-O-Cu]<sup>2+</sup> active site, and NO can greatly reduce the energy barrier for the conversion of the active site from [Cu-O-Cu]<sup>2+</sup> to the binuclear Cu form, while NO<sub>2</sub> can be slightly reduced. Through discussion, it is found that the binuclear Cu-ZSM-5 can realize the combined removal of N<sub>2</sub>O and NO<sub>x</sub> from adipic acid flue gas, hoping to provide a theoretical basis for the development of a dual-functional catalyst.



**Citation:** Gao, C.; Li, J.; Zhang, J.; Sun, X. DFT Study on the Combined Catalytic Removal of N<sub>2</sub>O, NO, and NO<sub>2</sub> over Binuclear Cu-ZSM-5. *Catalysts* **2022**, *12*, 438. <https://doi.org/10.3390/catal12040438>

Academic Editors: Anton Naydenov and C. Heath Turner

Received: 25 January 2022

Accepted: 9 April 2022

Published: 13 April 2022

**Publisher's Note:** MDPI stays neutral with regard to jurisdictional claims in published maps and institutional affiliations.



**Copyright:** © 2022 by the authors. Licensee MDPI, Basel, Switzerland. This article is an open access article distributed under the terms and conditions of the Creative Commons Attribution (CC BY) license (<https://creativecommons.org/licenses/by/4.0/>).

**Keywords:** binuclear Cu-ZSM-5; DFT; N<sub>2</sub>O decomposition; NO<sub>x</sub>-NH<sub>3</sub>-SCR; reaction mechanism

## 1. Introduction

The problems of global climate change and environmental pollution have seriously threatened the safety of human existence [1,2]. Nitrogen oxides (N<sub>2</sub>O, NO, NO<sub>2</sub>, etc.) exhausted in the bulk chemicals production [3,4] are the most important air pollutants and severely damage the environment [5,6]. As an important bulk chemical, adipic acid (C<sub>6</sub>H<sub>10</sub>O<sub>4</sub>) is a raw material that produces nylon 66 and polyurethane, and is widely used in chemical production, the organic synthesis industry, lubricants, medicine, dyes, and other fields. In 2020, the global adipic acid production capacity was 4.6 million tons, and the number is expected to be 4.8 million tons by 2022 [7]. Each ton of adipic acid produced releases 0.4 tons of mixed flue gas containing nitrogen oxides of which the proportion of N<sub>2</sub>O reaches 40%, and contains a small amount of NO and NO<sub>2</sub> (3000–4000 mg/m<sup>3</sup>) [8]. At present, the most common method for processing these nitrogen oxide mixed gases in industrial production is a two-step method—the first reactor performs catalytic decomposition of N<sub>2</sub>O, and then the second reactor undergoes NO and NO<sub>2</sub> (abbreviated as NO<sub>x</sub>) selective catalytic reduction (SCR). The development of a one-step process for simultaneously treating multiple nitrogen oxides in a single reactor can greatly reduce the production costs and the generation of secondary pollutants. Thus, it will be of incomparable significance to synthesize a dual-functional catalyst while simultaneously catalyzing the decomposition of N<sub>2</sub>O and reducing NO<sub>x</sub>.

Many studies have focused on the catalytic decomposition of N<sub>2</sub>O and NO<sub>x</sub>-NH<sub>3</sub>-SCR over M-exchanged (M = Fe, Cu, Ce, Mn, etc.) zeolites [9–24]. Smeets et al. [22] compared

the catalytic processes of different Cu-exchanging zeolites (BEA, MFI, FER, FAU, and MOR) during the  $N_2O$  decomposition. They put forward a kinetic model by analyzing the relevant elementary reaction steps and recognized that the speed-limiting step is the process of recombination of two O atoms into molecular  $O_2$ . Li et al. [23] combined experiments with DFT methods to study the  $NO_x$ - $NH_3$ -SCR reaction over Cu-SAPO-18 and found that there are two reaction routes (the standard SCR and the fast SCR routes). They proposed that when following the standard SCR reaction route, NO needs to be oxidized to produce  $NO_2$  and then react with  $NH_3$ . This step has a higher energy barrier; thus, the reaction speed is lower than when  $NO_2$  directly participates in the reaction according to the fast SCR route. Ariel et al. [21] studied the decomposition of  $N_2O$  and the  $NH_3$  catalytic reduction of  $N_2O$  and  $N_2O + NO$  over Fe-Z (Z = BEA, ZSM-5, and FER). They reported the yield of “oxo-species” ( $\alpha$ -oxygen) during the decomposition of  $N_2O$  and proved that the presence of NO greatly promotes the decomposition of  $N_2O$ . Colombo et al. [24] presented a systematic discussion on the mechanism of the  $NO/NO_2/N_2O-NH_3$  SCR over Fe-exchanged zeolite. They found that when equimolar amounts of NO and  $NO_2$  were added to the reactor, the highest deNO<sub>x</sub> activity was observed due to the fast SCR reaction. In addition, their data proved that NO oxidation activity is enhanced due to the presence of  $N_2O$ , thus emphasizing the interaction between  $N_2O$  reactivity and  $NH_3$ -SCR reaction.

Since Iwamoto et al. [25] proved that Cu-ZSM-5 has particularly excellent catalytic performance for NO catalytic decomposition, the outstanding catalytic ability for  $N_2O$  decomposition and  $NO_x$  SCR of Cu-ZSM-5 is gradually recognized [11,13,14,26–29]. It is generally believed that Cu-ZSM-5 contains a variety of catalytic active sites (such as mono-, bi-, and trinuclear Cu active sites) [30–33]. By adjusting the catalyst synthesis method, the position of the framework Al atoms and the main type of the catalytic active sites can be controlled [34–36]. The experimental conclusion of Salama et al. [9] showed that both the main channel and the sinusoidal channel of ZSM-5 zeolite can be used as the positions of Al atom pairs in the framework and load metal ions to form the catalytic active sites. The reports of spectroscopy, structure, and computational studies [11,37–39] found that the binuclear Cu active site can form the  $[Cu-O-Cu]^{2+}$  active site under the activation of  $O_2$  and  $N_2O$ . Woertink et al. [38] and Li et al. [40] pointed out that the  $[Cu-O-Cu]^{2+}$  site is the most stable species when the  $O_2$  partial pressure is relatively low and has high catalytic activity for direct oxidation of methane to methanol. The  $[Fe-O-Fe]^{2+}$  active site at the same position in the ZSM-5 catalyst is also analyzed by Sazama et al. [9], and they found that the  $[Fe-O-Fe]^{2+}$  site has remarkably high catalytic activity for  $NO_x$ - $NH_3$ -SCR. However, Cu-ZSM-5 is rarely reported for the combined removal of  $N_2O$  and  $NO_x$ - $NH_3$ -SCR at the same time.

In the present work, we sequentially calculate the decomposition process of  $N_2O$  over the binuclear Cu active site in the sinusoidal channel of Cu-ZSM-5 (abbreviated as binuclear Cu-ZSM-5) and the process of  $NO_x$ - $NH_3$ -SCR over the  $[Cu-O-Cu]^{2+}$  site. At the same time, the role of the addition of NO and  $NO_2$  in the conversion process between binuclear Cu site and the  $[Cu-O-Cu]^{2+}$  is briefly analyzed. Through a comprehensive analysis of the above reaction processes, we propose the possibility of coupling removal of  $N_2O$  and  $NO_x$  contained in adipic acid flue gas over the binuclear Cu-ZSM-5, which can provide a theoretical basis for the design and development of the dual-functional Cu-ZSM-5 catalyst.

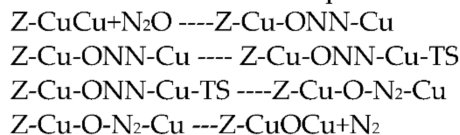
## 2. Results

### 2.1. $N_2O$ Direct Catalytic Decomposition Mechanism over Binuclear Cu-ZSM-5

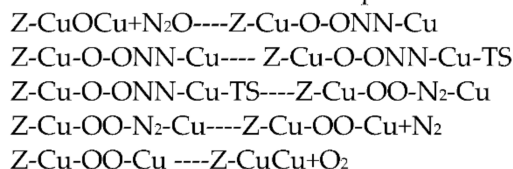
Based on Liu et al.'s [41] report on the decomposition of  $N_2O$  over the binuclear Cu site in the main channel and our previous research [42] over the mononuclear Cu-ZSM-5, we proposed the  $N_2O$  decomposition mechanism over the binuclear Cu active site in the sinusoidal channel (see Scheme 1). To simplify the description, the first  $N_2O$  molecule is noted as O1–N1–N2. The second  $N_2O$  molecule is labelled as O2–N3–N4. The energy profile of the decomposition process of two  $N_2O$  molecules and the key structural parameters of

each state are shown in Figure 1, and the detailed optimized geometric parameters for each state are listed in Table S1.

Part A1: The first N<sub>2</sub>O decomposition



Part A2: The second N<sub>2</sub>O decomposition



Overall:  $2\text{N}_2\text{O} \rightarrow 2\text{N}_2 + \text{O}_2$

**Scheme 1.** Reaction steps of N<sub>2</sub>O catalytic decomposition over the binuclear Cu active sites.

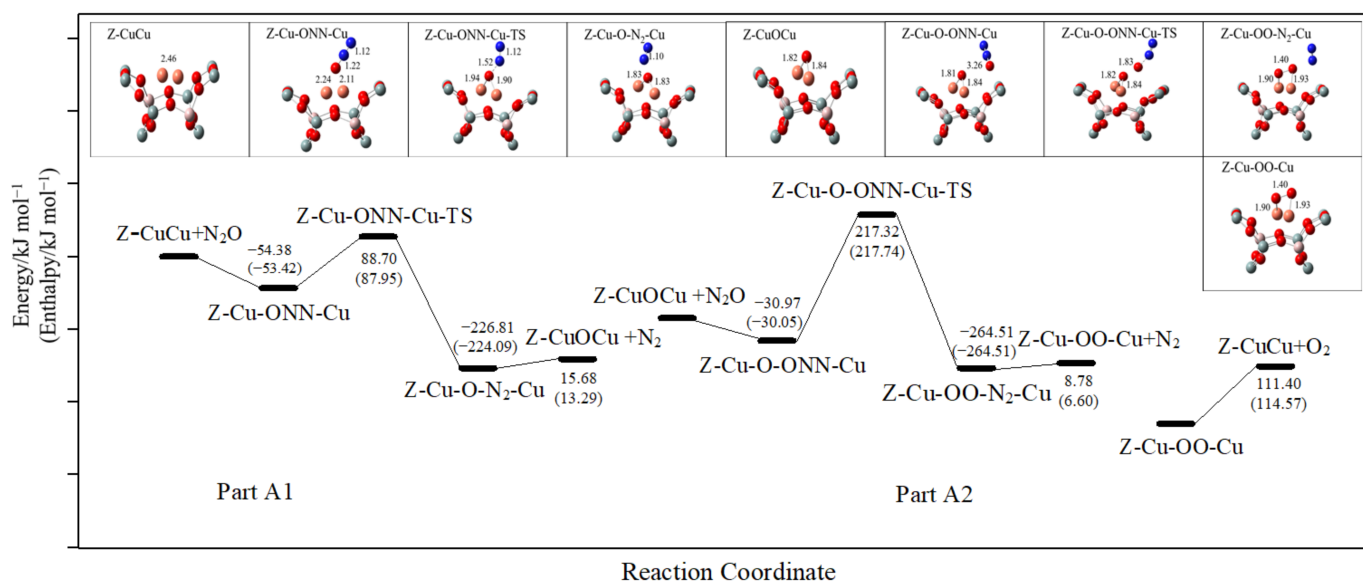


**Figure 1.** The energy profile of the reaction process of two N<sub>2</sub>O molecules catalytic decomposition. (The H atoms in the framework are omitted).

### 2.1.1. The First N<sub>2</sub>O Molecular Decomposition Process (Part A1)

As shown in Scheme 1, the decomposition of the first N<sub>2</sub>O molecule include four elementary steps. The first N<sub>2</sub>O molecule is adsorbed between two Cu atoms, forming an O-bridge with two Cu atoms. The distance between O1 atom and Cu1 atom is 2.11 Å, and the distance between O1 and Cu2 is 2.24 Å. The activation energy of the transition state Z-Cu-ONN-Cu-TS is 88.70 kJ mol<sup>-1</sup>, and the imaginary frequency is -680.84 cm<sup>-1</sup>. The distance between the O1 and the two Cu atoms in the transition state is reduced. The formation of the intermediate product Z-Cu-O-N<sub>2</sub>-Cu releases a lot of energy. The adsorbed N<sub>2</sub> desorbs from the active site and forms gaseous N<sub>2</sub>, and the intermediate product Z-CuOCu produced at the same time has a stable oxygen bridge structure, a process which only needs to absorb a small amount of energy ( $\Delta E = 15.68$  kJ mol<sup>-1</sup>). The triplet state of the Z-CuOCu structure is the most stable, which is consistent with the results of previous studies [38,40].

### 2.1.2. The Second N<sub>2</sub>O Molecular Decomposition Process (Part A2)

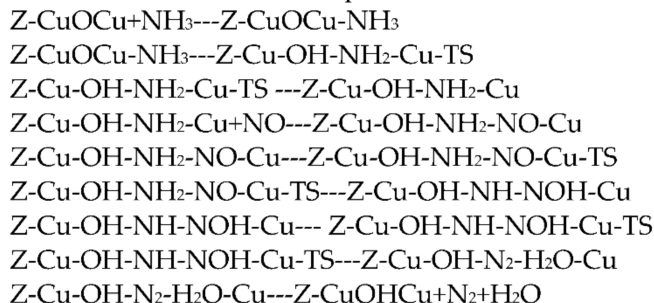
To realize the catalytic cycle, the second N<sub>2</sub>O molecule decomposes over the active site and releases N<sub>2</sub> and O<sub>2</sub>, and the binuclear Cu active site is regenerated. The second N<sub>2</sub>O

molecule is adsorbed on one side (Cu2) of the oxygen bridge structure. Since the adsorption energy of this step is small ( $-30.97 \text{ kJ mol}^{-1}$ ), the adsorption process is reversible. The activation energy of the transition state (Z-Cu-O-ONN-Cu-TS) is  $217.32 \text{ kJ mol}^{-1}$ ; the imaginary frequency of the transition state is  $-749.52 \text{ icm}^{-1}$ . This step has the highest reaction energy barrier and the slowest reaction rate; thus, it can be regarded as the rate-limiting step for the decomposition of two molecules of  $\text{N}_2\text{O}$ . Subsequently, the O2-N3 bond of the intermediate product (Z-Cu-OO-N<sub>2</sub>-Cu) breaks, the two O atoms form a four-membered ring structure with Cu1 and Cu2, and an adsorbed  $\text{N}_2$  generates at the same time. The step from the transition state (Z-Cu-O-ONN-Cu-TS) to the intermediate product (Z-Cu-OO-N<sub>2</sub>-Cu) releases a lot of energy, leading to the automatic desorption of  $\text{N}_2$  and  $\text{O}_2$  in the next two steps.

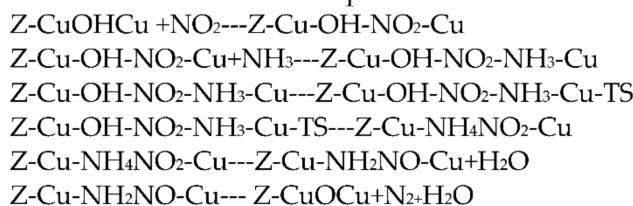
## 2.2. $\text{NO}_x\text{-NH}_3\text{-SCR}$ Mechanism over the $[\text{Cu-O-Cu}]^{2+}$ Active Site

The intermediate product, Z-CuOCu, during the first  $\text{N}_2\text{O}$  molecular decomposition process has a stable extra-framework  $[\text{Cu-O-Cu}]^{2+}$  structure, which is proved by Li [40] and his team, suggesting that it can be used as the active site for the  $\text{CH}_4$  selective oxidation, and the  $[\text{Cu-O-Cu}]^{2+}$  structure is the most stable under the condition of low  $\text{O}_2$  partial pressure. The  $[\text{Fe-O-Fe}]^{2+}$  active site (similar to the Z-CuOCu) was proved by Sazama et al. [9] to have very great  $\text{NO}_x\text{-NH}_3\text{-SCR}$  catalytic efficiency. Based on the research conclusions of Zhou et al. [43], Boubnov et al. [44], Chen et al. [45], Li et al. [46], and Zhao et al. [47] on the reaction mechanism of  $\text{NO}_x\text{-NH}_3\text{-SCR}$ , we proposed the elementary steps of  $\text{NO}_x\text{-NH}_3\text{-SCR}$  over the  $[\text{Cu-O-Cu}]^{2+}$  active site (as shown in Scheme 2). The energy profile of the  $\text{NO}_x\text{-NH}_3\text{-SCR}$  process and the key structural parameters of each state are shown in Figure 2, and the detailed optimized geometric parameters for each state are listed in Tables S2 and S3.

### Part B1: The $\text{NO}$ and $\text{NH}_3\text{SCR}$ process



### Part B2: The $\text{NO}_2$ and $\text{NH}_3\text{SCR}$ process



**Scheme 2.** Reaction steps of  $\text{NO}_x\text{-NH}_3\text{-SCR}$  over  $[\text{Cu-O-Cu}]^{2+}$  active site.

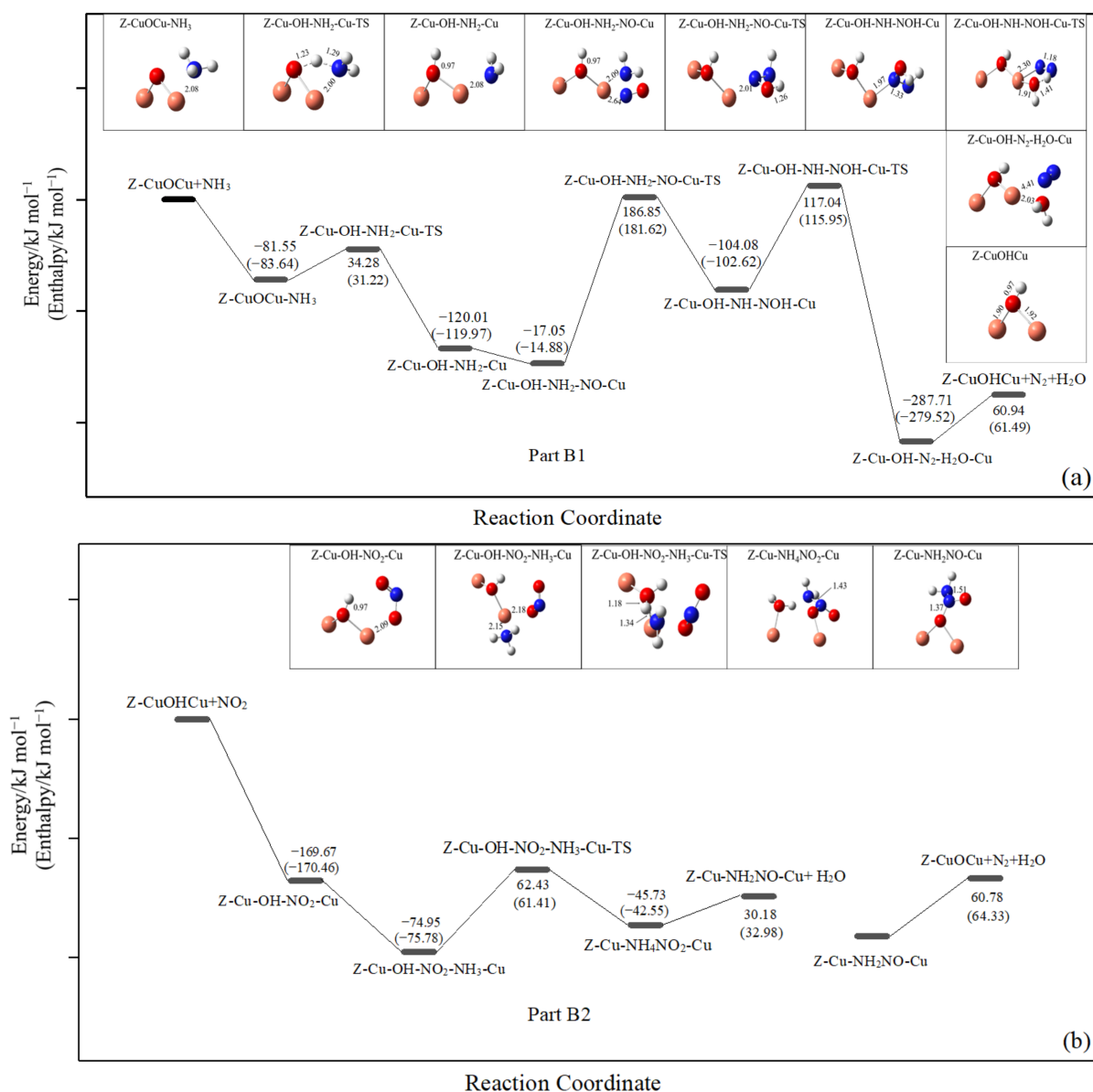


**Figure 2.** The energy profile of the reaction steps of NO<sub>x</sub>-NH<sub>3</sub>-SCR over the [Cu-O-Cu]<sup>2+</sup> active site: (a) the reaction of NO and NH<sub>3</sub>, (b) the reaction of NO<sub>2</sub> and NH<sub>3</sub>. (All the framework atoms are omitted.)

### 2.2.1. The NO and NH<sub>3</sub>-SCR Process (Part B1)

Much of the literature [43] claimed that the adsorption of NH<sub>3</sub> on the Cu-zeolite active site is stronger than that of NO. However, there is no report on the adsorption of NO and NH<sub>3</sub> over the [Cu-O-Cu]<sup>2+</sup> active site in the sinusoidal channel. By calculation we found that NH<sub>3</sub> is adsorbed on the Z-CuOCu active site earlier than NO, and this process can be considered as the first step of the NO-NH<sub>3</sub>-SCR reaction. After the NH<sub>3</sub> is adsorbed, the adsorption state (Z-CuOCu-NH<sub>3</sub>) absorbs 34.28 kJ mol<sup>-1</sup> energy to generate the transition state (Z-Cu-OH-NH<sub>2</sub>-Cu-TS). During this process, the N-H bond of NH<sub>3</sub> breaks, and an O-H bond forms between the O atom of the active site and the H atom from the NH<sub>3</sub>. The imaginary frequency of the transition state is  $-1464.52 \text{ icm}^{-1}$ . Subsequently, NO adsorbs into the reaction system and releases a small amount of energy (17.05 kJ mol<sup>-1</sup>). During the formation of the second transition state (Z-Cu-OH-NH<sub>2</sub>-NO-Cu-TS), the distance between NH<sub>2</sub> and Cu<sub>2</sub> increases, the N atom of the NO forms a N-Cu<sub>2</sub> bond, a N-N bond is formed between the two N atoms, and the O atom of NO competes for another H atom of the NH<sub>2</sub> cluster. The imaginary frequency of the second transition state is  $-1807.70 \text{ icm}^{-1}$ . As the

rate-limiting step in the NO-NH<sub>3</sub>-SCR process, in this step, energy barrier reaches up to 186.85 kJ mol<sup>-1</sup>. During the generation of the third transition state (Z-Cu-OH-NH-NOH-Cu-TS), the NH<sub>3</sub> loses the third H atom and forms an adsorbed H<sub>2</sub>O and an adsorbed N<sub>2</sub>. The virtual frequency of the third transition state structure is -227.97 icm<sup>-1</sup>, and the energy barrier of this process is 117.04 kJ mol<sup>-1</sup>. Due to the large amount of energy released during the generation of the intermediate product (Z-Cu-OH-N<sub>2</sub>-H<sub>2</sub>O-Cu), the N<sub>2</sub> and H<sub>2</sub>O can be spontaneously desorbed from the active site. The whole NO-NH<sub>3</sub>-SCR process is shown in Part B1 of Figure 2a.

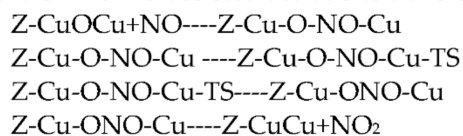
### 2.2.2. The NO<sub>2</sub> and NH<sub>3</sub>-SCR Process (Part B2)

The NO<sub>2</sub> is adsorbed first and then followed by the NH<sub>3</sub>. The NO<sub>2</sub> molecule adsorbs on the Cu<sub>2</sub> with the O-terminal, the Cu<sub>2</sub>-O1 bond length is 2.09 Å, and the adsorption energy value is -169.67 kJ mol<sup>-1</sup>. The NH<sub>3</sub> is adsorbed on the same Cu atom (Cu<sub>2</sub>) as NO<sub>2</sub>. The bond length of the Cu<sub>2</sub>-N2 in the adsorbed product (Z-Cu-OH-NO<sub>2</sub>-NH<sub>3</sub>-Cu) is 2.15 Å, the bond length of Cu<sub>2</sub>-O2 increases to 2.18 Å, and the adsorption energy value is -74.95 kJ mol<sup>-1</sup>. In the transition state Z-Cu-OH-NO<sub>2</sub>-NH<sub>3</sub>-Cu-TS, one of the H atoms of the NH<sub>3</sub> resonates with the O atom, and the distance between the two N atoms of NO<sub>2</sub> and NH<sub>3</sub> is also shortened. The virtual frequency of the transition state is -877.90 icm<sup>-1</sup>, and the energy barrier of this step is 62.43 kJ mol<sup>-1</sup>, which is the rate-limiting step of the NO<sub>2</sub> and NH<sub>3</sub> SCR process. After the N-H bond is broken and a N-N bond is formed, an adsorbed H<sub>2</sub>O and an NH<sub>2</sub>NO cluster are formed in the intermediate product Z-Cu-NH<sub>4</sub>NO<sub>2</sub>-Cu. We have discussed the evolution of the specific structure from the NH<sub>2</sub>NO cluster to N<sub>2</sub> and H<sub>2</sub>O in Part B1, so this part will not be repeated, and the NH<sub>2</sub>NO cluster is treated as a whole set. After the H<sub>2</sub>O and N<sub>2</sub> cluster desorb from the active site in turn, the catalyst active site returned to the clean catalyst surface, which is the binuclear Cu state (Z-CuCu). The structure and energy data are listed in Part B2 of Figure 2b.

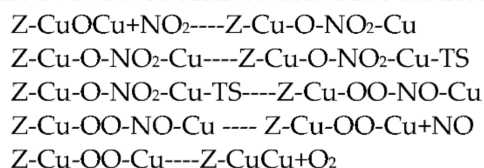
### 2.3. The NO<sub>x</sub>-Assisted Active Site Transformation Process

When the first N<sub>2</sub>O molecule decomposes over the binuclear Cu(Z-CuCu) and releases N<sub>2</sub>, the catalytic active site turns into [Cu-O-Cu]<sup>2+</sup>(Z-CuOCu). Previous reports [37,48–53] pointed out that NO can improve the catalytic efficiency of N<sub>2</sub>O decomposition because NO as a potential oxygen carrier can remove the O atom of the active site easily. Therefore, Part C and Part D discuss the reaction process of NO and NO<sub>2</sub> promoting the migration of the active site from Z-CuOCu to Z-CuCu. Additionally, the mechanisms of the active site transformation assisted by NO and NO<sub>2</sub> are proposed as below (shown in Scheme 3). The energy profile of the NO<sub>x</sub>-assisted active site transformation process and the key structural parameters of each state are shown in Figure 3, and the detailed optimized geometric parameters for each state are listed in Table S4.

#### Part C: The NO-assisted active site transformation process



#### Part D: The NO<sub>2</sub>-assisted active site transformation process



**Scheme 3.** Reaction pathways for the NO<sub>x</sub>-assisted active site transformation process.

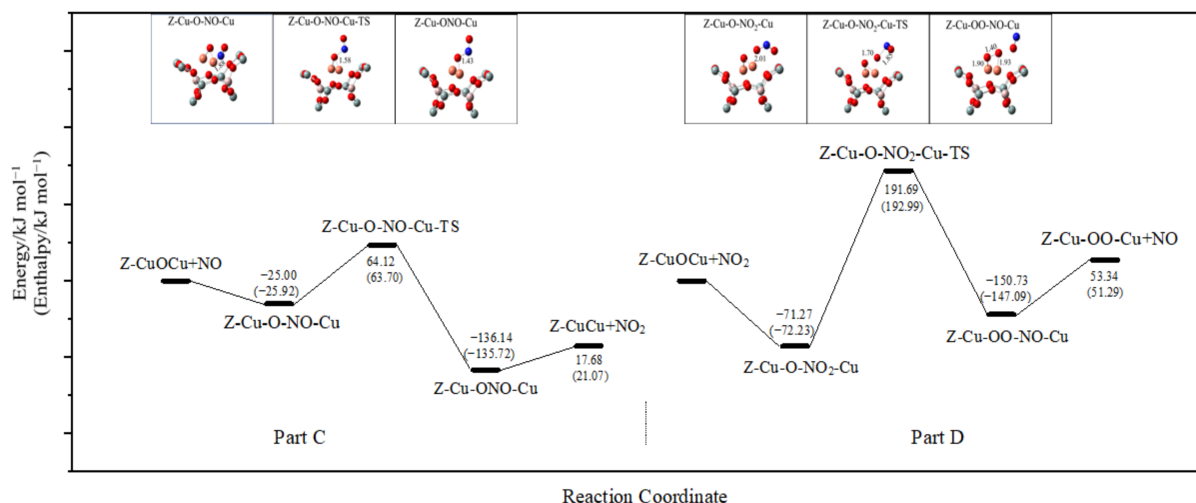


**Figure 3.** The energy profile of the reaction process of  $\text{NO}_x$ -assisted active site transformation. (The H atoms in the framework are omitted.)

### 2.3.1. The NO-Assisted Active Site Transformation Process

Since NO is added into the  $\text{N}_2\text{O}$  decomposition system, the NO molecule adsorbs on the active site by the N-terminal (shown in Figure 3) and catches the O atom of the catalytic site to form the transition state (Z-Cu-O-NO-Cu-TS). The transition state energy barrier is  $64.12 \text{ kJ mol}^{-1}$ , and the virtual frequency is  $-468.28 \text{ icm}^{-1}$ . Subsequently, NO reacts with the O atom to generate  $\text{NO}_2$ , and then the  $\text{NO}_2$  is desorbed from the active site after absorbing  $17.68 \text{ kJ mol}^{-1}$  energy. It can be seen from Part C of Figure 3 that the NO activation process is the rate-limiting step of the NO-assisted active center transformation process, and the energy barrier is much smaller than that of the decomposition process of the  $\text{N}_2\text{O}$  molecule adsorbing on the same active site.

### 2.3.2. The $\text{NO}_2$ -Assisted Active Site Transformation Process

$\text{NO}_2$  is adsorbed on Cu2 with the O end (shown in Figure 3), and the adsorption energy is  $-71.27 \text{ kJ mol}^{-1}$ . The O2-Cu2 bond length of the adsorption product Z-Cu-O- $\text{NO}_2$ -Cu is  $2.01 \text{ \AA}$ . Then, the O atom of  $\text{NO}_2$  resonates with the N atom to form the transition state (Z-Cu-O- $\text{NO}_2$ -Cu-TS). The imaginary frequency of the transition state is  $-824.52 \text{ icm}^{-1}$ . This step is the rate-limiting step of the  $\text{NO}_2$ -assisted active center transformation process. The intermediate product Z-Cu-OO-NO-Cu has a four-membered ring structure (formed by the two Cu atoms and the two O atoms) and an adsorbed NO molecule. When the gaseous NO is desorbed from the system, the structure of Z-Cu-OO-Cu is the same as that of the intermediate product Z-Cu-OO-Cu in the second  $\text{N}_2\text{O}$  decomposition process (shown in Figure 1).

## 3. Discussion

The difference of the species and the location of the catalytic active sites in the catalyst will lead to the difference of the catalytic reaction pathway. Experimental and DFT calculations [38,39,54,55] have proved that there are multiple binuclear Cu active sites in the Cu-ZSM-5 catalyst that can be used for  $\text{N}_2\text{O}$  decomposition, and the most active sites are those where the two Cu distance is sufficiently short. Liu et al. [41] investigated the  $\text{N}_2\text{O}$  decomposition over the binuclear Cu active site in the main channel (the distance of two Cu atoms is  $3.36 \text{ \AA}$ ), applying experimental research and the same DFT simulation calculations as ours. In our previous work [42], we employed the DFT method to investigate the  $\text{N}_2\text{O}$  catalytic decomposition over the mononuclear Cu-ZSM-5. In the present work, we chose the binuclear Cu site in the sinusoidal channel (the distance of two Cu atoms is  $2.46 \text{ \AA}$ ) as the active site to discuss the catalytic decomposition process of two molecules of  $\text{N}_2\text{O}$  and found that the energy data of the related process are significantly different from that of

the mononuclear Cu active site or that of the binuclear Cu active site in the main channel. Table 1 shows the energy data of two N<sub>2</sub>O decomposition over various active sites. In the present work, the first N<sub>2</sub>O molecule adsorption energy value (−54.38 kJ mol<sup>−1</sup>) calculated is very consistent with the result reported by Tai et al. [39] in the study of the [Cu-O-Cu]<sup>2+</sup> active site formation (45.98 ± 8 kJ mol<sup>−1</sup>). The activation energy of N<sub>2</sub>O (88.70 kJ mol<sup>−1</sup>) is consistent with the reported [30] activation energy (about 75.24 kJ mol<sup>−1</sup>) obtained by the decomposition of N<sub>2</sub>O over the binuclear Cu active site. By comparing the energy data in Table 1, it can be found that on the mononuclear Cu active site, the process of O<sub>2</sub> desorption is the rate-limiting step, and the N<sub>2</sub>O decomposition reaction is inhibited by O<sub>2</sub>. However, on the binuclear Cu active site (both in the main channel and in the sinusoidal channel), the O<sub>2</sub> desorption process is not the rate-limiting step, and the reaction is not inhibited by O<sub>2</sub>. Through experimental studies, Smeets et al. [22] and Liu et al. [41] confirmed that when the Cu load increases, the active sites exist of Cu-ZSM-5 as the binuclear Cu form, and the N<sub>2</sub>O decomposition process is not inhibited by O<sub>2</sub>. Their experimental result is consistent with our theoretical conclusion. It can also be found in Table 1 that the first N<sub>2</sub>O decomposition over the binuclear Cu active site in the sinusoidal channel has the lowest activation energy. According to experiments and calculations, Tsai et al. [39] pointed out that when strong Cu-O-Cu bonds are formed, a larger thermodynamic driving force is generated, thereby reducing the activation energy. Over the binuclear Cu active site in the sinusoidal channel, the first N<sub>2</sub>O molecule exhibits the lowest activation energy, indicating that the [Cu-O-Cu]<sup>2+</sup> site in the sinusoidal channel has the highest stability, which is consistent with the conclusions reported by Li et al. [40] and Goodman et al. [33].

**Table 1.** Energy data of two N<sub>2</sub>O decomposition over various active sites.

		Energy (kJ mol <sup>−1</sup> )		
		Mononuclear [42]	Binuclear [41] Site in Main Channel	Present
The first N <sub>2</sub> O decomposition	N <sub>2</sub> O adsorption	−42.30	−203.52	−54.38
	Activation energy	138.27	197.25	88.70
The second N <sub>2</sub> O decomposition	N <sub>2</sub> O adsorption	−13.25	−192.11	−30.97
	Activation energy	119.59	267.06	217.32
	O <sub>2</sub> desorption	140.41	61.45	111.40

There are two types of SCR mechanisms: the standard SCR and the fast SCR. In the fast SCR mechanism, NO<sub>2</sub> directly participates in the reduction process, avoiding the higher energy barrier of the NO oxidation process in the standard SCR mechanism, and therefore, exhibits a higher reaction rate. Colombo et al. [24] tested the activity of a series of NO/NO<sub>2</sub> and NH<sub>3</sub> reactions with different component ratios. They proved that when NO and NO<sub>2</sub> participate in the reaction in equal amounts (NO<sub>2</sub>/NO<sub>x</sub> = 0.5), the SCR reaction shows the best deNO<sub>x</sub> performance, which is attributed to the fast SCR reaction mechanism. In the present work, after the first N<sub>2</sub>O decomposition process, a stable extra-frame [Cu-O-Cu]<sup>2+</sup> structure generates. We simulated the reaction mechanism of NO<sub>x</sub>-NH<sub>3</sub>-fast SCR over the [Cu-O-Cu]<sup>2+</sup> site by the DFT method. To simplify the description of the entire reaction process, the fast SCR reaction mechanism is selected for discussion. Colombo et al. [24] pointed out that the interaction between NH<sub>3</sub> and the catalyst active site is very important in the SCR reaction because the deNO<sub>x</sub> performance and the kinetics of the SCR converter are controlled by the reactivity of adsorbed NH<sub>3</sub>. Through many experimental results and simulation research data, Li et al. [23,46]. and Denis et al. [56] concluded that NH<sub>3</sub> in all reactants will first be adsorbed on the active site. This conclusion is reconfirmed by our current work. After the NH<sub>3</sub> is adsorbed on the active site, the dissociation of NH<sub>3</sub> to NH<sub>2</sub> occurs first, then the NH<sub>2</sub> reacts with the adsorbed NO to form a NH<sub>2</sub>NO cluster. The decomposition of the NH<sub>2</sub>NO cluster into H<sub>2</sub>O and N<sub>2</sub> (shown in Figure 2a, Part B1) has a relatively high activation energy. The same phenomenon was also confirmed by

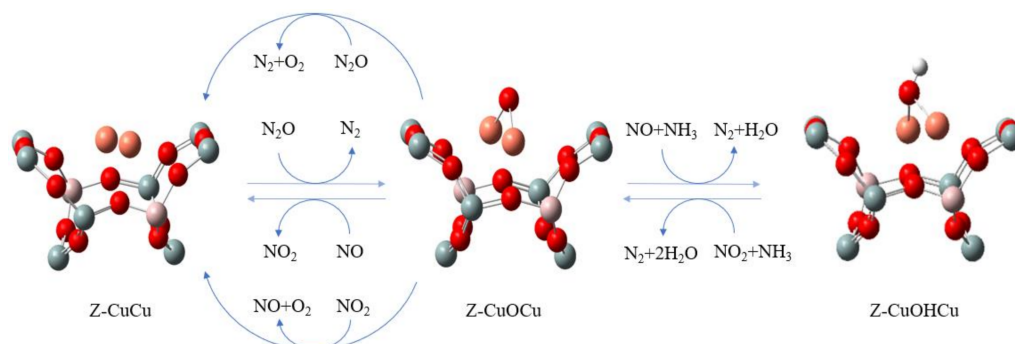
Mao et al. [57] while studying the  $\text{NO}_x\text{-NH}_3\text{-SCR}$  reaction on Cu-SAPO-34. They noted that an unstable, four-membered ring is formed during the intramolecular proton transfer, resulting in a strong steric hindrance. The mechanism of  $\text{NO}_2\text{-NH}_3\text{-SCR}$  is controversial in the literature. Based on transient reactivity experiments, Grossale et al. [58] pointed out that during the  $\text{NO}_2\text{-SCR}$  reaction, nitrates are formed as an important intermediate through the disproportionation of  $\text{NO}_2$ , then selectively reduced by  $\text{NH}_3$ . Iwasaki and Shinjoh [59] mentioned that a  $\text{NH}_3$  reacts with  $\text{NO}_2$  to form  $\text{N}_2\text{O}$  first, then the intermediate product  $\text{N}_2\text{O}$  reacts with another  $\text{NH}_3$ , and the sum of these two steps come to the stoichiometry of the  $\text{NO}_2\text{-SCR}$ . Colombo et al. [24] via a kinetic study and direct experimental evidence, proved that if the two-step mechanism is followed ( $\text{NO}_2$  is reduced to  $\text{N}_2\text{O}$  first), it is kinetically limited by the  $\text{N}_2\text{O}$  reduction process and therefore, damaging to the overall activity, which is inconsistent with their experimental evidence. This proves that the introduction of an independent  $\text{NO}_2\text{-SCR}$  reaction is feasible. Therefore, the  $\text{NO}_2\text{-NH}_3\text{-SCR}$  mechanism and simulation data listed can be a reference provided for readers. The rate of the entire  $\text{NO}_2\text{-NH}_3\text{-SCR}$  process is limited by the step that  $\text{NH}_3$  decomposes to form  $\text{NH}_2$ .

Smeets et al. [37] proved that  $\text{NO}$  can remove the O atom deposited by the  $\text{N}_2\text{O}$  decomposition process and form an adsorbed  $\text{NO}_2$ . After the  $\text{NO}_2$  is desorbed, an empty Cu site is regenerated, which can accept the new O atom from another  $\text{N}_2\text{O}$  molecule. Björn et al. [52,53] reported the same oxygen-carrier role of  $\text{NO}$  during the  $\text{NO}$  decomposition over Cu-ZSM-5. Based on previous work, we discussed the oxygen-carrying effect of  $\text{NO}$  over the active site of the  $[\text{Cu-O-Cu}]^{2+}$  and meanwhile, proposed a mechanism of  $\text{NO}_2$ -assisted active site transformation. We prove that both  $\text{NO}$  and  $\text{NO}_2$  can directly react over the  $[\text{Cu-O-Cu}]^{2+}$  active site and then take the O atom away to reduce the active site to the binuclear Cu form. Morpurgo [30,55] studied the mechanisms of  $\text{NO}$  and  $\text{N}_2\text{O}$  decomposition over the short-distance Cu pairs in Cu-ZSM-5. He proved that the decomposition of  $\text{N}_2\text{O}$  and  $\text{NO}$  can be achieved on short-distance Cu pairs and that  $\text{NO}$  has a promoting effect on the reduction of  $[\text{Cu-O-Cu}]^{2+}$  active sites. Morpurgo [30] studied the role of  $\text{NO}_2$  in the reduction of  $[\text{Cu-O-Cu}]^{2+}$  active site and reported that the activation energy of  $\text{NO}_2$  is  $173.47 \text{ kJ mol}^{-1}$ , which is particularly close to our calculate energy value ( $191.69 \text{ kJ mol}^{-1}$ ). In addition, according to his simulation conclusions, the O-bridge of the  $[\text{Cu-O-Cu}]^{2+}$  is easily destroyed by reacting with  $\text{NO}$ , but the decomposition of  $\text{NO}_2$  is slower because of the higher energy barrier. This conclusion is supported by our calculation results.

Table 2 summarizes the energy data of the key steps of all reactions that occurred over the  $[\text{Cu-O-Cu}]^{2+}$  active site in the present work. By comparison, it can be found that  $\text{NO}_x\text{-NH}_3\text{-SCR}$  has the lowest first step adsorption energy and can occur preferentially. After the  $\text{NO}_x\text{-NH}_3\text{-SCR}$  catalytic cycle is completed, the  $[\text{Cu-O-Cu}]^{2+}$  active site is regenerated. The flue gas of industrial adipic acid production contains a large amount of  $\text{N}_2\text{O}$  and a relatively small amount of  $\text{NO}$  and  $\text{NO}_2$ , and only a small amount of  $\text{NH}_3$  needs to be introduced into the system for the  $\text{NO}_x$  removal. Therefore, the occupancy of the active site by the  $\text{NO}_x\text{-NH}_3\text{-SCR}$  process does not affect the adsorption and decomposition of the second  $\text{N}_2\text{O}$  molecule over the  $[\text{Cu-O-Cu}]^{2+}$  active site. The rate-limiting step of the catalytic decomposition of  $\text{N}_2\text{O}$  over the binuclear Cu-ZSM-5 is the activation of the second  $\text{N}_2\text{O}$  molecule. When  $\text{NO}$  and  $\text{NO}_2$  are introduced, they can effectively accelerate the regeneration of the binuclear Cu active site. Combining the above reaction paths, it is theoretically feasible to realize the combined removal of  $\text{N}_2\text{O}$  and  $\text{NO}_x$  contained in adipic acid flue gas over the binuclear Cu active site in the sinusoidal channel, and the proposed catalytic cycle is shown in Figure 4.

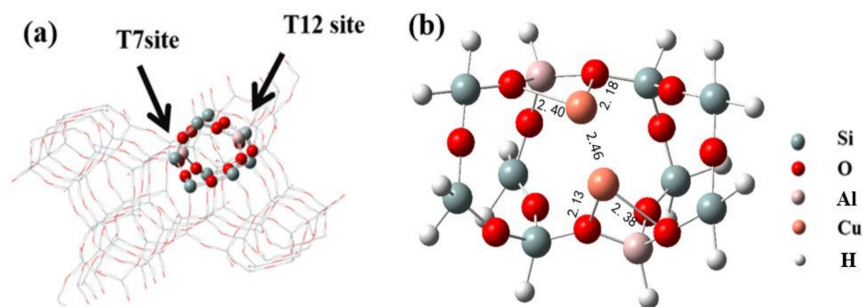
**Table 2.** Energy data of each reaction over the  $[\text{Cu-O-Cu}]^{2+}$  active site.

$\Delta E/\text{kJ}\cdot\text{mol}^{-1}$	Second $\text{N}_2\text{O}$ Decomposition	NO-Assisted	$\text{NO}_2$ -Assisted	$\text{NO}_x\text{-NH}_3\text{-SCR}$
Adsorption	−30.97	−25.00	−71.27	−81.55
Active energy of the first transition state	217.32	64.12	191.69	34.28
Energy barrier of rate-limiting step	217.32	64.12	191.69	186.85

**Figure 4.** The catalytic cycle of the combined removal of  $\text{N}_2\text{O}$  and  $\text{NO}_x$  over binuclear Cu-ZSM-5 (The H atoms in the framework are omitted.).

#### 4. Computational Methods and Model

In the present work, the density functional theory (DFT) method is applied to theoretically study the catalytic decomposition of  $\text{N}_2\text{O}$  and  $\text{NO}_x\text{-NH}_3\text{-SCR}$ . The structure of the ZSM-5 catalyst is intercepted from the database of the Material Studio software. The T7 and T12 sites in the sinusoidal channel of the ZSM-5 catalyst are chosen to introduce the extra-framework structure (See Figure 5a). These two sites are widely reported to be very suitable for the substitution of the multi-nuclear transition metal [40,60,61]. Figure 5b shows the optimized model of the binuclear Cu-ZSM-5 cluster  $[\text{Si}_8\text{Al}_{12}\text{O}_{12}\text{H}_{16}\text{Cu}_2]$ . After intercepting the binuclear Cu-ZSM-5 cluster model, the broken chemical bonds are supplemented by H atoms [18,62,63]. The structural parameters of the binuclear Cu-ZSM-5 model are highly consistent with those reported by Goodman et al. [33], and the distance between two Cu atoms is 2.46 Å, which is consistent with the reported results (2.48 Å).

**Figure 5.** (a) Location of the T7 and T12 positions in the sinusoidal channel of the ZSM-5 catalyst; (b) optimized binuclear Cu-ZSM-5 cluster.

All simulation calculations are based on the Gaussian-09 software package [41,63–65]. We simulate each state model based on the B3LYP method [66–69]. We chose the 6-311++G\*\* basis set for the Al, Si, N, O, and H atoms and the SDD basis set for the Cu atoms [40,56,70]. All the framework Si and O atoms are fixed, and other atoms are relaxed [62,71,72]. All singlet and triplet spin states are calculated using the broken-symmetry approach [38,39], and the one showing lower single-point energy is chosen [41,62]. All transition state

structures have been verified by the IRC theory, and all energy values have been corrected by zero-point energy [27,41,42,63].

To simplify the presentation, the binuclear Cu-ZSM-5 zeolite is abbreviated as Z-2Cu, and the transition state in each step is marked with TS. The Cu loaded at the T12 position is labelled as Cu1, and the Cu loaded at the T7 position is noted as Cu2.

## 5. Conclusions

In the present work, the binuclear Cu in the sinusoidal channel is selected as the active site to discuss the decomposition of two N<sub>2</sub>O molecules. At the same time, based on the [Cu-O-Cu]<sup>2+</sup> active site generated after the decomposition of the first N<sub>2</sub>O molecule, the NO<sub>x</sub>-NH<sub>3</sub>-SCR, the NO and the NO<sub>2</sub> decomposition mechanisms are studied. The relevant structural parameters of the reactant, products, and the energy barriers of all reaction transition states have been detailed on SI.

The results indicate that N<sub>2</sub>O can be catalytically decomposed over the binuclear Cu active site in the sinusoidal channel. However, the second N<sub>2</sub>O molecule will not decompose easily, and this process will be the rate-limiting step in the whole reaction. After the decomposition of the first N<sub>2</sub>O molecule, a stable extra-frame [Cu-O-Cu]<sup>2+</sup> structure generates. The subsequent discussion proved that the NO<sub>x</sub>-NH<sub>3</sub>-SCR reaction can be realized over the [Cu-O-Cu]<sup>2+</sup> active center. In addition, the NO can greatly reduce the energy barrier for the conversion of the active site from the [Cu-O-Cu]<sup>2+</sup> form to the binuclear Cu form, while the NO<sub>2</sub> can slightly reduce. Through a comprehensive comparison and discussion, it was proven that the combined removal of N<sub>2</sub>O and NO<sub>x</sub> contained in adipic acid flue gas can be achieved over the binuclear Cu-ZSM-5 in the sinusoidal channel, and the corresponding catalytic cycle is proposed.

**Supplementary Materials:** The following supporting information can be downloaded at: <https://www.mdpi.com/article/10.3390/catal12040438/s1>, Table S1: Structural parameters of optimized models in the N<sub>2</sub>O decomposition process; Table S2: Structural parameters of optimized models in the NO-NH<sub>3</sub>-SCR process; Table S3: Structural parameters of optimized models in the NO<sub>2</sub>-NH<sub>3</sub>-SCR process; Table S4: Structural parameters of optimized models of NO<sub>x</sub>-assisted reduction of active site.

**Author Contributions:** Writing—original draft preparation, C.G.; supervision, J.L.; writing—review and editing, J.Z.; methodology, X.S. All authors have read and agreed to the published version of the manuscript.

**Funding:** This research was funded by National Key Research and Development Project, grant number 2017YFC0210905.

**Data Availability Statement:** Not applicable.

**Conflicts of Interest:** The authors declare no conflict of interest.

## References

1. Manisalidis, I.; Stavropoulou, E.; Stavropoulos, A.; Bezirtzoglou, E. Environmental and Health Impacts of Air Pollution: A Review. *Front. Public Health* **2020**, *8*, 14. [[CrossRef](#)] [[PubMed](#)]
2. Ghorani-Azam, A.; Riahi-Zanjani, B.; Balali-Mood, M. Effects of air pollution on human health and practical measures for prevention in Iran. *J. Res. Med. Sci.* **2016**, *21*, 65. [[PubMed](#)]
3. Yan, W.; Zhang, G.; Wang, J.; Liu, M.; Sun, Y.; Zhou, Z.; Zhang, W.; Zhang, S.; Xu, X.; Shen, J.; et al. Recent Progress in Adipic Acid Synthesis Over Heterogeneous Catalysts. *Front. Chem.* **2020**, *8*, 185–197. [[CrossRef](#)]
4. Liu, L.; Zhu, J.; Zhang, Y.; Chen, X. An Optimal Pollution Control Model for Environmental Protection Cooperation between Developing and Developed Countries. *Int. J. Environ. Res. Public Health* **2020**, *17*, 3868–3888. [[CrossRef](#)] [[PubMed](#)]
5. Schreiber, F.; Wunderlin, P.; Udert, K.; Wells, G. Nitric oxide and nitrous oxide turnover in natural and engineered microbial communities: Biological pathways, chemical reactions, and novel technologies. *Front. Microbiol.* **2012**, *3*, 372. [[CrossRef](#)] [[PubMed](#)]
6. Ritz, B.; Hoffmann, B.; Peters, A. The Effects of Fine Dust, Ozone, and Nitrogen Dioxide on Health. *Dtsch. Arztebl. Int.* **2019**, *116*, 881–886. [[CrossRef](#)] [[PubMed](#)]
7. Analysis of the Supply and Demand Status of the Global Adipic Acid Industry Market in 2021. Available online: <https://ecoapp.qianzhan.com/> (accessed on 14 March 2022).

8. Hongyu, L. Study on Cooperative Catalytic Exhaust Mulyi-Pollutants in the Flue Gas of Adipic Acid Production. Master's Thesis, Beijing University of Chemical Technology, Beijing, China, 2019.
9. Sazama, P.; Wichterlová, B.; Tábor, E.; Šťastný, P.; Sathu, N.K.; Sobalík, Z.; Dědeček, J.; Sklenák, Š.; Klein, P.; Vondrová, A. Tailoring of the structure of Fe-cationic species in Fe-ZSM-5 by distribution of Al atoms in the framework for N<sub>2</sub>O decomposition and NH<sub>3</sub>-SCR-NO<sub>x</sub>. *J. Catal.* **2014**, *312*, 123–138. [[CrossRef](#)]
10. Wang, J.; Xia, H.; Ju, X.; Fan, F.; Feng, Z.; Li, C. Catalytic performance of different types of iron zeolites in N<sub>2</sub>O decomposition. *Chin. J. Catal.* **2013**, *34*, 876–888. [[CrossRef](#)]
11. Groothaert, M.H.; Lievens, K.; Leeman, H.; Weckhuysen, B.M.; Schoonheydt, R.A. An operando optical fiber UV-vis spectroscopic study of the catalytic decomposition of NO and N<sub>2</sub>O over Cu-ZSM-5. *J. Catal.* **2003**, *220*, 500–512. [[CrossRef](#)]
12. Chen, L.; Chen, H.Y.; Lin, J.; Tan, K.L. FTIR, XPS and TPR studies of N<sub>2</sub>O decomposition over Cu-ZSM-5. *Surf. Interface Anal.* **1999**, *28*, 115–118. [[CrossRef](#)]
13. Zou, W.; Xie, P.; Hua, W.; Wang, Y.; Kong, D.; Yue, Y.; Ma, Z.; Yang, W.; Gao, Z. Catalytic decomposition of N<sub>2</sub>O over Cu-ZSM-5 nanosheets. *J. Mol. Catal. A Chem.* **2014**, *394*, 83–88. [[CrossRef](#)]
14. Meng, T.; Ren, N.; Ma, Z. Silicalite-1@Cu-ZSM-5 core-shell catalyst for N<sub>2</sub>O decomposition. *J. Mol. Catal. A Chem.* **2015**, *404–405*, 233–239. [[CrossRef](#)]
15. Li, G.; Pidko, E.A.; Pilot, I.A.W.; van Santen, R.A.; Li, C.; Hensen, E.J.M. Catalytic properties of extraframework iron-containing species in ZSM-5 for N<sub>2</sub>O decomposition. *J. Catal.* **2013**, *308*, 386–397. [[CrossRef](#)]
16. Zhang, B.; He, G.; Shan, Y.; He, H. Experimental and DFT study of the adsorption of N<sub>2</sub>O on transition ion-exchanged ZSM-5. *Catal. Today* **2019**, *327*, 177–181. [[CrossRef](#)]
17. Ates, A. Characteristics of Fe-exchanged natural zeolites for the decomposition of N<sub>2</sub>O and its selective catalytic reduction with NH<sub>3</sub>. *Appl. Catal. B Environ.* **2007**, *76*, 282–290. [[CrossRef](#)]
18. Liu, N.; Zhang, R.; Chen, B.; Li, Y.; Li, Y. Comparative study on the direct decomposition of nitrous oxide over M (Fe, Co, Cu)–BEA zeolites. *J. Catal.* **2012**, *294*, 99–112. [[CrossRef](#)]
19. Yakovlev, A.L.; Zhidomirov, G.M.; van Santen, R.A. N<sub>2</sub>O Decomposition Catalysed by Transition Metal Ions. *Catal. Lett.* **2001**, *75*, 45–48. [[CrossRef](#)]
20. Zhou, T.; Liu, S.; Tang, M.; Chen, C.; Xu, Y.; Wu, J. Progress on selective catalytic reduction de-NO<sub>x</sub> catalysts. *J. Chin. Ceram. Soc.* **2009**, *37*, 317–324.
21. Guzmanvargas, A. Catalytic decomposition of N<sub>2</sub>O and catalytic reduction of N<sub>2</sub>O and N<sub>2</sub>O + NO by NH<sub>3</sub> in the presence of O<sub>2</sub> over Fe-zeolite. *Appl. Catal. B Environ.* **2003**, *42*, 369–379. [[CrossRef](#)]
22. Smeets, P.; Sels, B.; Vanteffelen, R.; Leeman, H.; Hensen, E.; Schoonheydt, R. The catalytic performance of Cu-containing zeolites in N<sub>2</sub>O decomposition and the influence of O<sub>2</sub>, NO and H<sub>2</sub>O on recombination of oxygen. *J. Catal.* **2008**, *256*, 183–191. [[CrossRef](#)]
23. Li, Y.; Deng, J.; Song, W.; Liu, J.; Zhao, Z.; Gao, M.; Wei, Y.; Zhao, L. Nature of Cu Species in Cu–SAPO-18 Catalyst for NH<sub>3</sub>-SCR: Combination of Experiments and DFT Calculations. *J. Phys. Chem. C* **2016**, *120*, 14669–14680. [[CrossRef](#)]
24. Colombo, M.; Nova, I.; Tronconi, E.; Schmeißer, V.; Bandl-Konrad, B.; Zimmermann, L. NO/NO<sub>2</sub>/N<sub>2</sub>O–NH<sub>3</sub> SCR reactions over a commercial Fe-zeolite catalyst for diesel exhaust aftertreatment: Intrinsic kinetics and monolith converter modelling. *Appl. Catal. B Environ.* **2012**, *111–112*, 106–118. [[CrossRef](#)]
25. Iwamoto, M.; Yahiro, H.; Tanda, K.; Mizuno, N.; Mine, Y.; Kagawa, S. Removal of nitrogen monoxide through a novel catalytic process. 1. Decomposition on excessively copper-ion-exchanged ZSM-5 zeolites. *J. Phys. Chem.* **1991**, *95*, 3727–3730. [[CrossRef](#)]
26. Maity, P.; Yamazoe, S.; Tsukuda, T. Dendrimer-Encapsulated Copper Cluster as a Chemoselective and Regenerable Hydrogenation Catalyst. *ACS Catal.* **2013**, *3*, 182–185. [[CrossRef](#)]
27. Liu, X.; Yang, Z.; Zhang, R.; Li, Q.; Li, Y. Density Functional Theory Study of Mechanism of N<sub>2</sub>O Decomposition over Cu-ZSM-5 Zeolites. *J. Phys. Chem. C* **2012**, *116*, 20262–20268. [[CrossRef](#)]
28. Meng, T.; Ren, N.; Ma, Z. Effect of copper precursors on the catalytic performance of Cu-ZSM-5 catalysts in N<sub>2</sub>O decomposition. *Chin. J. Chem. Eng.* **2018**, *26*, 1051–1058. [[CrossRef](#)]
29. Izquierdo, R.; Rodríguez, L.J.; Añez, R.; Sierraalta, A. Direct catalytic decomposition of NO with Cu–ZSM-5: A DFT–ONIOM study. *J. Mol. Catal. A Chem.* **2011**, *348*, 55–62. [[CrossRef](#)]
30. Morpurgo, S. The mechanism of NO and N<sub>2</sub>O decomposition catalyzed by short-distance Cu(I) pairs in Cu-ZSM-5: A DFT study on the possible role of NO and NO<sub>2</sub> in the [Cu–O–Cu]<sup>2+</sup> active site reduction. *J. Catal.* **2018**, *366*, 189–201. [[CrossRef](#)]
31. Hamada, H.; Matsubayashi, N.; Shimada, H.; Kintaichi, Y.; Ito, T.; Nishijima, A. XANES and EXAFS analysis of copper ion-exchanged ZSM-5 zeolite catalyst used for nitrogen monoxide decomposition. *Catal. Lett.* **1990**, *5*, 189–196. [[CrossRef](#)]
32. Goodman, B.; Schneider, W.; Hass, K.; Adams, J. Theoretical analysis of oxygen-bridged Cu pairs in Cu-exchanged zeolites. *Catal. Lett.* **1998**, *56*, 183–188. [[CrossRef](#)]
33. Goodman, B.; Hass, K.; Schneider, W.; Adams, J. Cluster Model Studies of Oxygen-Bridged Cu Pairs in Cu-ZSM-5 Catalysts. *J. Phys. Chem. B* **1999**, *103*, 10452–10460. [[CrossRef](#)]
34. Dědeček, J.; Sobalík, Z.; Wichterlová, B. Siting and Distribution of Framework Aluminium Atoms in Silicon-Rich Zeolites and Impact on Catalysis. *Catal. Rev.* **2012**, *54*, 135–223. [[CrossRef](#)]
35. Sazama, P.; Dědeček, J.; Gábová, V.; Wichterlová, B.; Spoto, G.; Bordiga, S. Effect of aluminium distribution in the framework of ZSM-5 on hydrocarbon transformation. Cracking of 1-butene. *J. Catal.* **2008**, *254*, 180–189. [[CrossRef](#)]

36. Dedecek, J.; Balgová, V.; Pashkova, V.; Klein, P.; Wichterlová, B. Synthesis of ZSM-5 Zeolites with Defined Distribution of Al Atoms in the Framework and Multinuclear MAS NMR Analysis of the Control of Al Distribution. *Chem. Mater.* **2012**, *24*, 3231–3239. [[CrossRef](#)]
37. Smeets, P.J.; Groothaert, M.H.; van Teeffelen, R.M.; Leeman, H.; Hensen, E.J.M.; Schoonheydt, R.A. Direct NO and N<sub>2</sub>O decomposition and NO-assisted N<sub>2</sub>O decomposition over Cu-zeolites: Elucidating the influence of the CuCu distance on oxygen migration. *J. Catal.* **2007**, *245*, 358–368. [[CrossRef](#)]
38. Woertink, J.S.; Smeets, P.J.; Groothaert, M.H.; Vance, M.A.; Sels, B.F.; Schoonheydt, R.A.; Solomon, E.I. A [Cu<sub>2</sub>O]<sup>2+</sup> core in Cu-ZSM-5, the active site in the oxidation of methane to methanol. *Proc. Natl. Acad. Sci. USA* **2009**, *106*, 18908–18913. [[CrossRef](#)]
39. Tsai, M.L.; Hadt, R.G.; Vanelderen, P.; Sels, B.F.; Schoonheydt, R.A.; Solomon, E.I. [Cu<sub>2</sub>O]<sup>2+</sup> active site formation in Cu-ZSM-5: Geometric and electronic structure requirements for N<sub>2</sub>O activation. *J. Am. Chem. Soc.* **2014**, *136*, 3522–3529. [[CrossRef](#)]
40. Li, G.; Vassilev, P.; Sanchez-Sanchez, M.; Lercher, J.A.; Hensen, E.J.M.; Pidko, E.A. Stability and reactivity of copper oxo-clusters in ZSM-5 zeolite for selective methane oxidation to methanol. *J. Catal.* **2016**, *338*, 305–312. [[CrossRef](#)]
41. Liu, X.; Yang, Z.; Li, Y.; Zhang, F. Theoretical study of N<sub>2</sub>O decomposition mechanism over binuclear Cu-ZSM-5 zeolites. *J. Mol. Catal. A Chem.* **2015**, *396*, 181–187. [[CrossRef](#)]
42. Gao, C.; Li, J.; Zhang, J.; Sun, X. DFT Study on Mechanisms of the N<sub>2</sub>O Direct Catalytic Decomposition over Cu-ZSM-5: The Detailed Investigation on NO Formation Mechanism. *Catalysts* **2020**, *10*, 646. [[CrossRef](#)]
43. Zhou, G.; Zhong, B.; Wang, W.; Guan, X.; Huang, B.; Ye, D.; Wu, H. In situ DRIFTS study of NO reduction by NH<sub>3</sub> over Fe–Ce–Mn/ZSM-5 catalysts. *Catal. Today* **2011**, *175*, 157–163. [[CrossRef](#)]
44. Boubnov, A.; Carvalho, H.W.P.; Doronkin, D.E.; Guenter, T.; Gallo, E.; Atkins, A.J.; Jacob, C.R.; Grunwaldt, J.D. Selective catalytic reduction of NO over Fe-ZSM-5: Mechanistic insights by operando HERFD-XANES and valence-to-core X-ray emission spectroscopy. *J. Am. Chem. Soc.* **2014**, *136*, 13006. [[CrossRef](#)] [[PubMed](#)]
45. Chen, P.; Jabłońska, M.; Weide, P.; Caumanns, T.; Weirich, T.; Muhler, M.; Moos, R.; Palkovits, R.; Simon, U. Formation and Effect of NH<sup>4+</sup> Intermediates in NH<sub>3</sub>–SCR over Fe-ZSM-5 Zeolite Catalysts. *ACS Catal.* **2016**, *6*, 7696–7700. [[CrossRef](#)]
46. Li, J.; Li, S. A DFT Study toward Understanding the High Activity of Fe-Exchanged Zeolites for the “Fast” Selective Catalytic Reduction of Nitrogen Oxides with Ammonia. *J. Phys. Chem. C* **2008**, *112*, 16938–16944. [[CrossRef](#)]
47. Zhao, X.; Li, X.; Liu, Z.; Mu, W.; Wei, H. Insights into the mechanism for the selective catalytic reduction of NO<sub>x</sub> with NH<sub>3</sub> on (MnO)<sup>2+</sup>/ZSM-5: A DFT study. *J. Theor. Comput. Chem.* **2017**, *16*, 1750030. [[CrossRef](#)]
48. Mul, G.; Pérez-Ramírez, J.; Kapteijn, F.; Moulijn, J.A. NO-Assisted N<sub>2</sub>O Decomposition over ex-Framework FeZSM-5: Mechanistic Aspects. *Catal. Lett.* **2001**, *77*, 7–13. [[CrossRef](#)]
49. Pérez-Ramírez, J.; Kapteijn, F.; Mul, G.; Moulijn, J.A. NO-Assisted N<sub>2</sub>O Decomposition over Fe-Based Catalysts: Effects of Gas-Phase Composition and Catalyst Constitution. *J. Catal.* **2002**, *208*, 211–223. [[CrossRef](#)]
50. Sang, C.; Lund, C.R.F. Possible role of nitrite/nitrate redox cycles in N<sub>2</sub>O decomposition and light-off over Fe-ZSM-5. *Catal. Lett.* **2001**, *73*, 73–77. [[CrossRef](#)]
51. Sang, C.; Kim, B.H.; Lund, C.R.F. Effect of NO upon N<sub>2</sub>O Decomposition over Fe/ZSM-5 with Low Iron Loading. *J. Phys. Chem. B* **2005**, *109*, 2295–2301. [[CrossRef](#)]
52. Modén, B.; Da Costa, P.; Fonfó, B.; Lee, D.K.; Iglesia, E. Kinetics and Mechanism of Steady-State Catalytic NO Decomposition Reactions on Cu–ZSM5. *J. Catal.* **2002**, *209*, 75–86. [[CrossRef](#)]
53. Modén, B.; Da Costa, P.; Lee, D.K.; Iglesia, E. Transient Studies of Oxygen Removal Pathways and Catalytic Redox Cycles during NO Decomposition on Cu–ZSM5. *J. Phys. Chem. B* **2002**, *106*, 9633–9641. [[CrossRef](#)]
54. Groothaert, M.H.; van Bokhoven, J.A.; Battiston, A.A.; Weckhuysen, B.M.; Schoonheydt, R.A. Bis(μ-oxo)dicopper in Cu-ZSM-5 and Its Role in the Decomposition of NO: A Combined in Situ XAFS, UV–Vis–Near-IR, and Kinetic Study. *J. Am. Chem. Soc.* **2003**, *125*, 7629–7640. [[CrossRef](#)] [[PubMed](#)]
55. Morpurgo, S. A DFT study on the mechanism of NO decomposition catalyzed by short-distance Cu(I) pairs in Cu-ZSM-5. *Mol. Catal.* **2017**, *434*, 96–105. [[CrossRef](#)]
56. Denis, P.; Ventura, O.; Le, H.; Nguyen, M. Density functional study of the decomposition pathways of nitroethane and 2-nitropropane. *Phys. Chem. Chem. Phys.* **2003**, *5*, 1730–1738.
57. Mao, Y.; Wang, Z.; Wang, H.-F.; Hu, P. Understanding catalytic reactions over zeolites: A density functional theory study of selective catalytic reduction of NO<sub>x</sub> by NH<sub>3</sub> over Cu-SAPO-34. *ACS Catalysis* **2016**, *6*, 7882–7891. [[CrossRef](#)]
58. Grossale, A.; Nova, I.; Tronconi, E. Ammonia blocking of the “Fast SCR” reactivity over a commercial Fe-zeolite catalyst for Diesel exhaust aftertreatment. *J. Catal.* **2009**, *265*, 141–147. [[CrossRef](#)]
59. Iwasaki, M.; Shinjoh, H. A comparative study of “standard”, “fast” and “NO<sub>2</sub>” SCR reactions over Fe/zeolite catalyst. *Appl. Catal. A Gen.* **2010**, *390*, 71–77. [[CrossRef](#)]
60. Li, G.; Pidko, E.A.; van Santen, R.A.; Li, C.; Hensen, E.J.M. Stability of Extraframework Iron-Containing Complexes in ZSM-5 Zeolite. *J. Phys. Chem. C* **2013**, *117*, 413–426. [[CrossRef](#)]
61. Pidko, E.A.; Hensen, E.J.M.; van Santen, R.A. Self-organization of extraframework cations in zeolites. *Proc. R. Soc. A Math. Phys. Eng. Sci.* **2012**, *468*, 2070–2086. [[CrossRef](#)]
62. Liu, X.; Zhang, J.; Huang, C.; Sun, X. Density Functional Theory Study of Cu-ZSM-5-Catalyzed C–H Bond Activation: The Importance of Active Centers. *J. Phys. Chem. C* **2018**, *122*, 28645–28651. [[CrossRef](#)]

63. Chen, B.; Liu, N.; Liu, X.; Zhang, R.; Li, Y.; Li, Y.; Sun, X. Study on the direct decomposition of nitrous oxide over Fe-beta zeolites: From experiment to theory. *Catal. Today* **2011**, *175*, 245–255. [[CrossRef](#)]
64. Frisch, M.; Trucks, G.; Schlegel, H.; Scuseria, G.; Robb, M.; Cheeseman, J.; Scalmani, G.; Barone, V.; Petersson, G.; Nakatsuji, H.; et al. *Gaussian 09, Revision D.01*; Gaussian Inc: Wallingford, CT, USA, 2016.
65. Joshi, A.M.; Delgass, W.N.; Thomson, K.T. Adsorption of Copper Clusters in TS-1 Pores: Ti versus Si and Gold versus Copper. *J. Phys. Chem. C* **2007**, *111*, 11888–11896. [[CrossRef](#)]
66. Becke, A.D. Density-functional exchange-energy approximation with correct asymptotic behavior. *Phys. Rev. A* **1988**, *38*, 3098–3100. [[CrossRef](#)] [[PubMed](#)]
67. Lee, C.; Yang, W.; Parr, R.G. Development of the Colle-Salvetti correlation-energy formula into a functional of the electron density. *Phys. Rev. B* **1988**, *37*, 785–789. [[CrossRef](#)] [[PubMed](#)]
68. Mota, A.J.; Cienfuegos, L.Á.d.; Robles, R.; Perea-Buceta, J.E.; Colacio, E.; Timón, V.; Hernández-Laguna, A. DFT approach to reaction mechanisms through molecular complexes. The case of an organo-catalysed nucleosidation reaction. *J. Mol. Struct.* **2010**, *944*, 43–52. [[CrossRef](#)]
69. Gomes, J.R.B.; Gomes, J.A.N.F. Adsorption of the formate species on copper surfaces: A DFT study. *Surf. Sci.* **1999**, *432*, 279–290. [[CrossRef](#)]
70. Kim, C.K.; Won, J.; Kim, H.S.; Kang, Y.S.; Li, H.G.; Kim, C.K. Density functional theory studies on the dissociation energies of metallic salts: Relationship between lattice and dissociation energies. *J. Comput. Chem.* **2001**, *22*, 827–834. [[CrossRef](#)]
71. Yakovlev, A.L.; Zhidomirov, G.M.; van Santen, R.A. DFT Calculations on N<sub>2</sub>O Decomposition by Binuclear Fe Complexes in Fe/ZSM-5. *J. Phys. Chem. B* **2001**, *105*, 12297–12302. [[CrossRef](#)]
72. He, M.; Zhang, J.; Sun, X.-L.; Chen, B.-H.; Wang, Y.-G. Theoretical Study on Methane Oxidation Catalyzed by Fe/ZSM-5: The Significant Role of Water on Binuclear Iron Active Sites. *J. Phys. Chem. C* **2016**, *120*, 27422–27429. [[CrossRef](#)]